

## Supporting Information

### **Chlorine-conducted defect repairment and seed crystal-mediated vapor growth process for controllable preparation of efficient and stable perovskite solar cells**

*Paifeng Luo,<sup>\*,†</sup> Zhaofan Liu,<sup>†</sup> Wei Xia,<sup>†</sup> Chenchen Yuan,<sup>‡</sup> Jigui Cheng,<sup>†</sup> Chenxi Xu,<sup>†</sup>  
Yingwei Lu<sup>†</sup>*

<sup>†</sup>Department of Materials Science and Engineering, Hefei University of Technology,  
Hefei, Anhui, 230009, P.R.China

<sup>‡</sup>CAS Key Laboratory of Materials for Energy Conversion, University of Science and  
Technology of China, Hefei, Anhui, 230026, P.R.China

\*E-mail: lpfeng@hfut.edu.cn

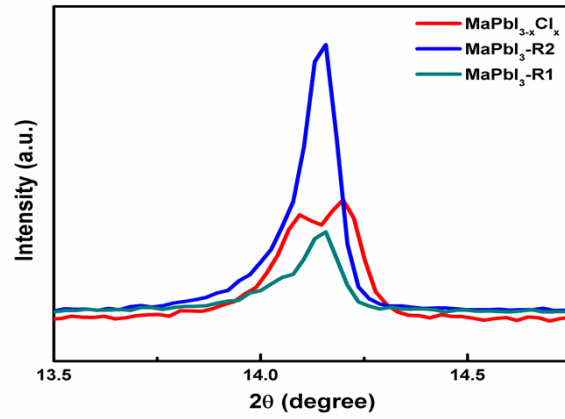


**Fig. S1** Enlarged XRD patterns of crystal plane (110).  $\text{MaPbI}_{3-x}\text{Cl}_x$  and  $\text{MaPbI}_3$  films by R2,  $\text{MaPbI}_3$  films by R1 are denoted by red line, blue line, and dark cyan line, respectively. As examined by XRD, the peak positions of  $\text{MaPbI}_3$  films by R1 and R2, and  $\text{MaPbI}_{3-x}\text{Cl}_x$  seed crystals are separately centered at  $14.06^\circ$ ,  $14.16^\circ$ , and  $14.20^\circ$ . With the increasing of Cl content, the peak position slightly shifts to a higher degree, and the full width at half maximum (FWHM) is broadened.

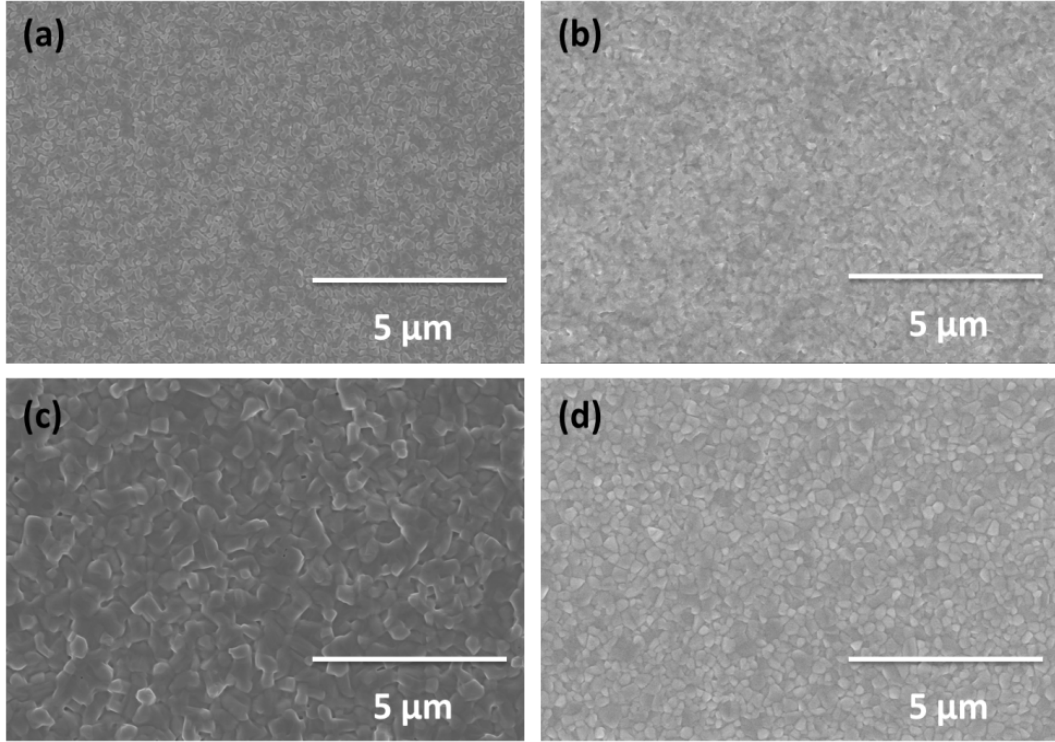


**Fig. S2** Planar SEM ( $\times 10$  K) images of (a)  $\text{PbI}_2$ , (b)  $\text{MaPbI}_{3-x}\text{Cl}_x$  and (c)  $\text{MaPbI}_3$  films by R2, and (d)  $\text{MaPbI}_3$  films by R1. From picture (a), we can see that  $\text{PbI}_2$  films are crisscrossed by irrigation canals and ditches, which should be the inherent ditch defects arising from the volatilization of DMF solvent. With the aid of  $\text{MaCl}$ , smooth, continuous, and closely packed  $\text{MaPbI}_{3-x}\text{Cl}_x$  seed crystal films with full coverage, as shown in picture (b), are generated. Finally, the compact, crack-free, and highly uniform  $\text{MaPbI}_3$  films with large grains visible in picture (c) are achieved by R2. From  $\text{MaPbI}_3$  films by R1 in picture (d), irregular small grains with obvious cracks are observed.

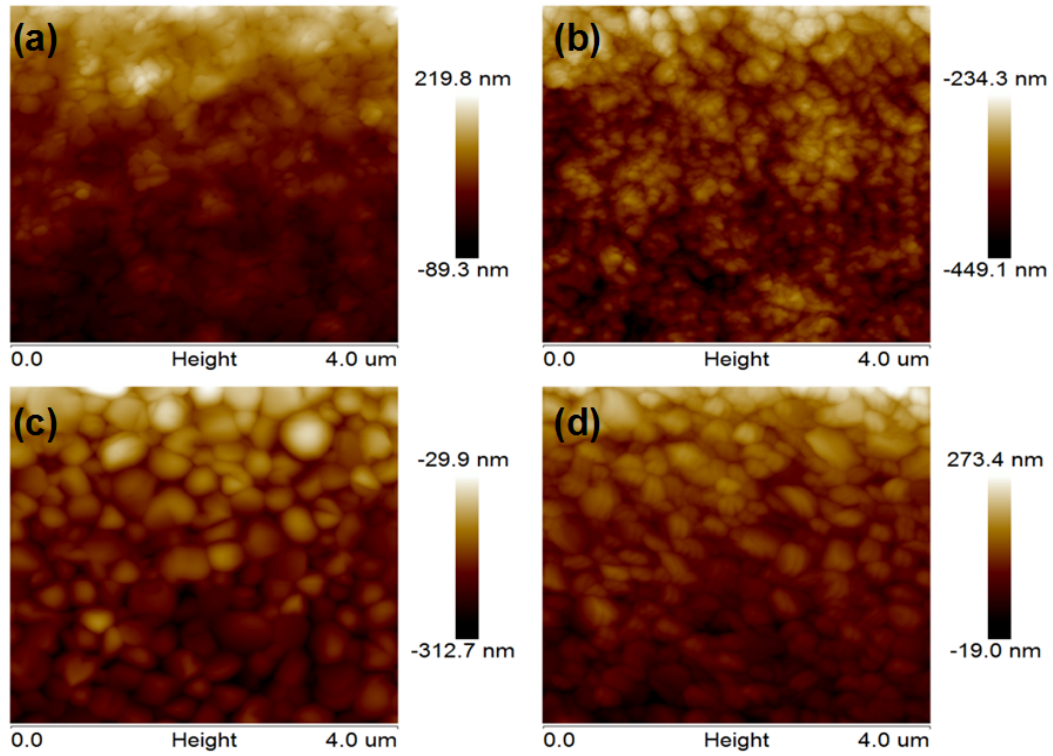


**Fig. S3** The 2-D height images ( $4 \times 4 \mu\text{m}$ ) of (a)  $\text{PbI}_2$ , (b)  $\text{MaPbI}_{3-x}\text{Cl}_x$  and (c)  $\text{MaPbI}_3$  films by R2, and (d)  $\text{MaPbI}_3$  films by R1. From images (a) and (b), we can clearly see the grain refining process, and the dith defects are sucessfully healed by the introduction of  $\text{MaCl}$ . From pictures (c) and (d), we can observe that grains via R2 are much larger and denser, and more uniform than that of by R1.

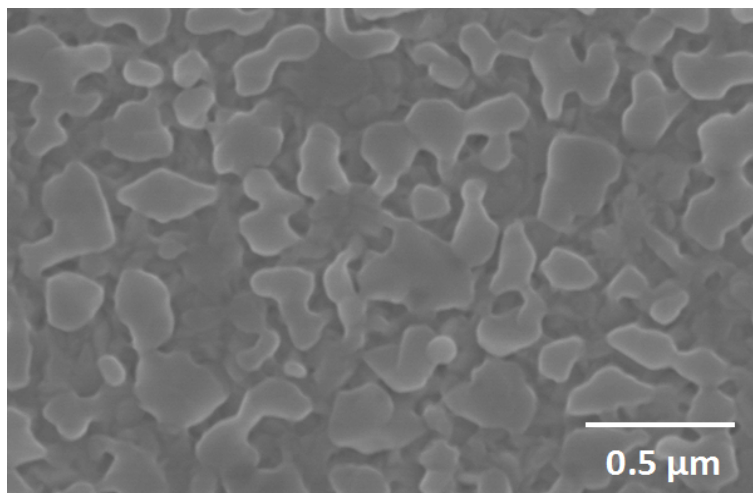


**Fig. S4** Planar SEM (  $\times 50$  K) images of PbI<sub>2</sub> films. Here we can see that irregular polyhedron shape grains with different sizes of 100~300 nm are randomly coated on the substrate. It is evident that the surface is crisscrossed by irrigation canals and ditches, and these inherent defects should be resulted from the volatilization of DMF solvent during the spin-coating and hot treatment process.

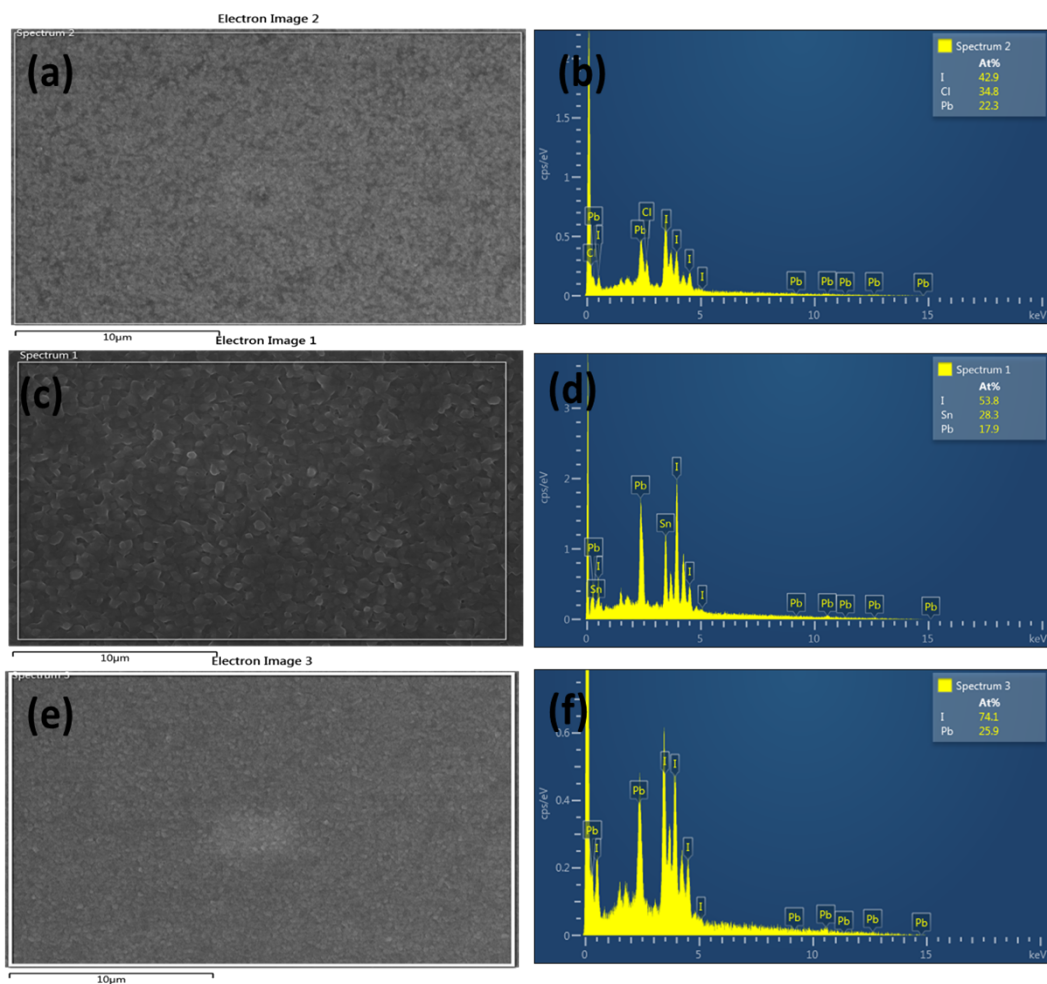


**Fig. S5** The SEM-EDS of (a, b) MaPbI<sub>3-x</sub>Cl<sub>x</sub>, (c, d) MaPbI<sub>3</sub> films by R2, and (e, f) MaPbI<sub>3</sub> films by R1. The ratio of I/Cl/Pb is close to 1.9:1.5:1 in MaPbI<sub>3-x</sub>Cl<sub>x</sub> films, and I/Pb ratios both in MaPbI<sub>3</sub> films by R2 and R1 are close to 3:1. Additionally, the detected Sn signal in picture (d) is caused by the FTO substrate.

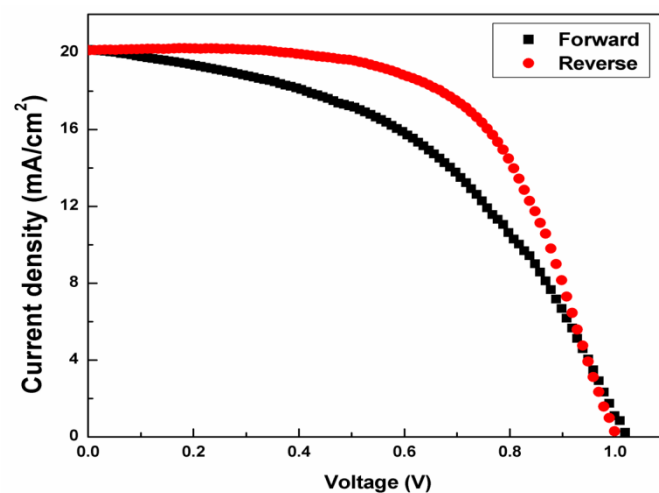


**Fig. S6** J-V curves of the perovskite solar cells with reverse and forward scan mode. Forward scan from -0.1V to 1.2V and reverse scan from 1.2V to -0.1V. The step voltage was fixed at 10mV. The PSCs in the reverse scan give the PCE of 12.29% with  $J_{sc}$  of 20.16 mA/cm<sup>2</sup>,  $V_{oc}$  of 1.002 V, and  $FF$  of 60.84%; PSCs in the forward scan give the PCE of 9.67% with  $J_{sc}$  of 20.25 mA/cm<sup>2</sup>,  $V_{oc}$  of 1.019 V, and  $FF$  of 46.86%.

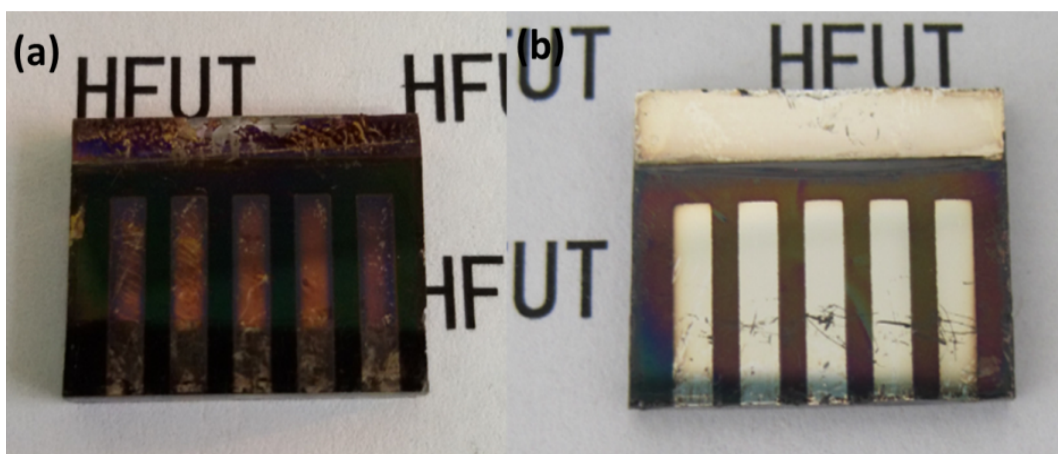


**Fig. S7** Picture of PSCs by (a) common CVD and (b) STCVD after stored for 48 days. We can obviously observe that the R1 device by common CVD is totally destroyed; while there is no apparent change in the appearance of R2 cells by STCVD.